Shahrood University of Technology

Journal of Mining and Environment (JME)

Journal homepage: www.jme.shahroodut.ac.ir

Iranian Society of Mining Engineering (IRSME)

Cyanide Removal from Tailing Slurry of Gold Processing Plant using Surfactant-modified Zeolite

Mehdi Soleymani Gharegol[1], Kazem Badv[1], and Behzad Nemati Akhgar[2]*

1. Civil Engineering Department, Engineering Faculty, Urmia University, Urmia, Iran, Iran
2. Mining Engineering Department, Engineering Faculty, Urmia University, Urmia, Iran

Article Info

Received 3 June 2023
Received in Revised form 22 October 2023
Accepted 1 November 2023
Published online 1 November 2023

DOI: 10.22044/jme.2023.13217.2418

Keywords

Cyanide
Surfactant
Adsorption isotherms
Kinetics
Gold tailings dam

Abstract

This paper carried out the study on removing cyanide from aqueous solutions by modified zeolite with hexadecyltrimethylammonium bromide. After determining the properties of the prepared adsorbent by the XRD, SEM, FTIR, and BET techniques, the effect of parameters such as the initial concentration of cyanide, pH, contact time, temperature, and the ionic strength of cyanide was examined by batch tests, and the effects of bed depth and flow rate on the performance of cyanide adsorption was investigated by column process. The XRD analysis showed the presence of clinoptilolite mineral in the structure of the raw zeolite, and the surface coating of raw zeolite by surfactant was detected by the SEM method. The FT-IR results confirmed the adsorption of cationic surfactant on the surface of the modified zeolite. The Langmuir, Freundlich and Tamkin adsorption models showed an excellent ability to describe the cyanide adsorption isotherm using the studied adsorbent. The adsorption capacity of cyanide by modified zeolite was 3.97 mg/g, significantly increased compared to the maximum adsorption capacity of raw zeolite cyanide (0.54 mg/g). The pseudo-second-order model has an excellent ability to describe the adsorption kinetics of cyanide contaminants using natural and modified zeolites. Maximum cyanide uptake capacity was achieved at pH value 8. Cyanide removal decreased with increasing pH and ionic strength of the stock solution and increased with an increase in solution temperature. Column study results confirmed that the adsorption capacity increased with the increasing bed depth, and decreased with increasing flow rate. Yoon-Nelson curves are closer to the experimental curves with high R2 values.

1. Introduction

Cyanide is a toxic pollutant that is widely released from industrial wastewater such as metal plating, drugs, and the food industry [1]. Cyanide has adverse effects on the health of humans and other living organisms, so exposure to small amounts of cyanide can be fatal. Water-soluble cyanide exists in two forms, free cyanide and cyanide complex [2]. Hydrogen cyanide is the most toxic type of cyanide, which is very important from an environmental perspective [3]. Contamination caused by tailing dams of mineral processing plants is one of the most important problems facing the mineral industry, and that causes many environmental problems. This wastewater contains significant amounts of cyanide and its compounds. Among the methods of removing cyanide from aqueous media are oxidation [4-5], adsorption [6-7], ion exchange [8-9], precipitation [10] and reverse osmosis [11-12], which in the oxidation method using an oxidant ion converts cyanide into low-risk compounds such as cyanate [13]. Economic and environmental considerations such as low-cost and non-production of toxic residues are the essential factors in choosing a method to remove cyanide from the solution. While most of these methods are costly, the adsorption method is considered an efficient method of economy, low waste production [14], ease of use, and usable for aqueous solutions containing medium or low concentrations of pollutants, and must be removed

Corresponding author: b.n.akhgar@urmia.ac.ir (B. Nemati Akhgar)

quickly. The adsorption process transfers components from a fluid and its accumulation in a solid adsorbent that continues until it reaches an equilibrium of the concentration of adsorbent components in the fluid and the surface adsorbent [15]. Low price, high abundance, and high capacity are the characteristics of a suitable adsorbent. The adsorption technique is studied in both batch and column tests. Most adsorption research works are carried out using a batch study utilizing adsorbate concentration, pH, temperature, contact time, etc., and column study using column height, flow rate, adsorbate concentration, etc. Various adsorbents such as activated carbon [16-17], activated carbon modified with iron [18], copper [19-20], zero-valent iron [21] and titanium dioxide [22] have been used to adsorb cyanide from aqueous solutions [1].

Recently, adsorption using zeolitic materials has attracted much attention in environmental applications [23-24]. Zeolites are crystalline compounds with a porous structure with very fine, orderly, and open pores consisting of a tetrahedral network of SiO_4 and AlO_4 [25]. Zeolites are generally natural and synthetic (synthesizable in the laboratory). Today, almost all natural species can be prepared in synthetic form. Applications of zeolite include adsorbent and catalyst in industry and research [26]. Clinoptilolite zeolite is a natural species of zeolite whose natural mines exist in Iran [27]. Zeolite, as an adsorbent, usually contain a negative charge. Therefore, they are less inclined to adsorb anionic species and are usually cation exchangers. Most adsorbents used to remove pollution from aqueous media have an acceptable capacity for cationic contaminants. The anionic property of cyanide in solution is the most critical barrier to using various materials with high adsorption capacity to eliminate cyanide toxicity. In general, zeolites contain a negative surface charge and, unlike cations, do not show much tendency to adsorb anions. One way to increase the adsorption capacity of anions by zeolite is to change their surface chemistry using different materials. Cationic surfactants are positively charged, and have an excellent ability to absorb anionic contaminants. One of the common types of surfactants to modify the surface of various materials is hexadecyltrimethylammonium bromide [25]. Manyuchi *et al.*, (2022) investigated the potential using biochar potential to remove heavy metals and cyanide from gold mining wastewater [28]. They showed that bioadsorbents can be successfully used to remove contaminants from gold tailings dam wastewater. Zhou *et al.*, (2023) did studies in the field on the removal of metal ions from cyanide gold extraction wastewater by alkaline ion-exchange fibers [29]. The results indicated that the adsorption efficiency of the cyanide complexes in practical wastewater reached 92% at a concentration of 30 g/L.

Because zeolites do not have the same adsorption behavior due to different origins and impurities in different places and due to the abundance of enormous zeolite mines and the high capacity of clinoptilolite ion exchange, and also because not many studies have been reported to study cyanide adsorption by zeolite, therefore, in this study, the efficiency of surface-modified zeolite in the West Azerbaijan Province with hexadecyltrimethylammonium bromide to absorb cyanide from aqueous solutions from the tailings of Zarshoran Takab gold mine processing plant was investigated. Based on this, the present study aimed to investigate the removal efficiency of cyanide from solution by surface-modified zeolite solutions. In the batch study, some parameters like the effect of solution pH on cyanide adsorption, contact time, the initial concentration and ionic strength of cyanide, and adsorption isotherms and kinetics were studied. Dynamic behavior of fixed-bed column was described in terms of the breakthrough curve. As part of this study, the effects of bed depth and flow rate on the performance of cyanide adsorption onto modified zeolite were investigated. The Yoon-Nelson model was used to compare the experimental data.

2. Materials and Methods

2.1. Geographical location

Zarshouran gold mine is located about 35 km from Takab and Shahin-Dez, West Azerbaijan Province, Iran. This mine is one of the most important ore deposits in this district, and is the biggest gold deposit in the Middle East (Figure 1) and belongs to the Iranian mines and mining industries development company. The method of gold extraction in this mine is cyanidation processing, which the effluent with a large amount of (free or complex) cyanide and its compounds finally enter the tailings dam.

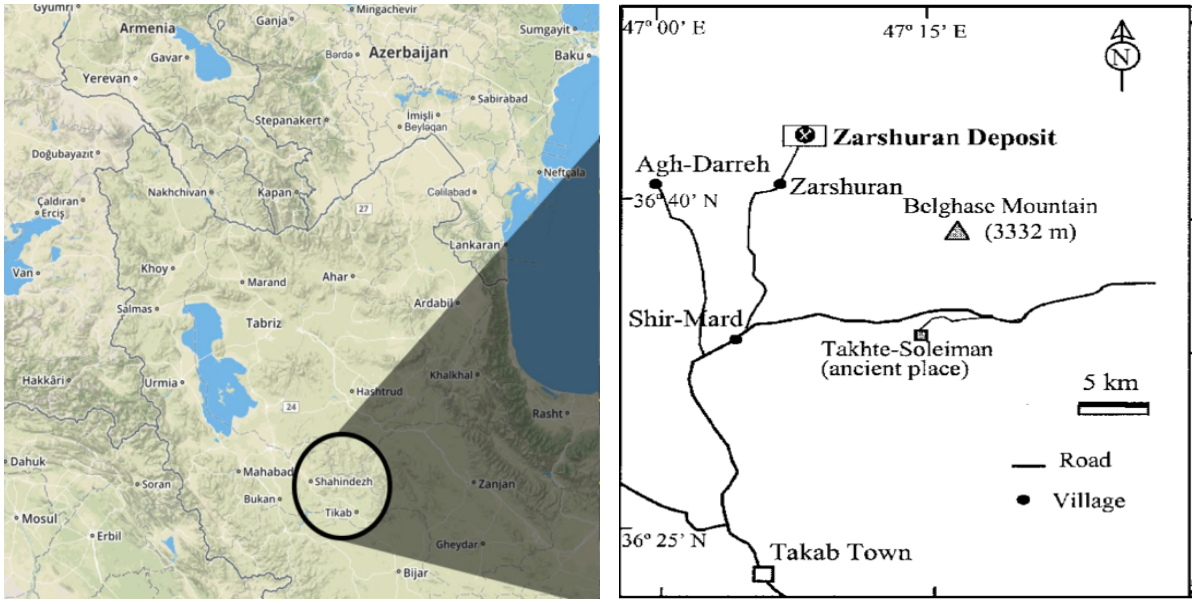

Figure 1. Location of Zarshouran gold mine.

2.2. Characterization of adsorbent and preparing

Natural zeolite (NZ) was prepared from the pozzolan mine of Qiz-Korpi Shahin-Dezh, located in the West Azerbaijan Province, Iran. The Qiz-Korpi Shahin-Dezh clinoptilolite is the most common natural zeolite belonging to the heulandite family. It has the following general formula: $KNa_2Ca_2(Si_{29}Al_7)\ O_{72}.24H_2O$ established from its X-ray diffraction (XRD) pattern. From the X-ray diffraction (XRD) data (Figure 2), SiO_2 by 70.46% was identified as a major phase component of the natural zeolite (NZ), with a small part of Al_2O_3 by 13.73%. The ratio of Si to Al (generally 4.0-5.3) (Kowalczyk *et al*., 2006) was 5.12 in the samples studied here. The chemical composition of natural zeolite (NZ) is shown in Table 1.

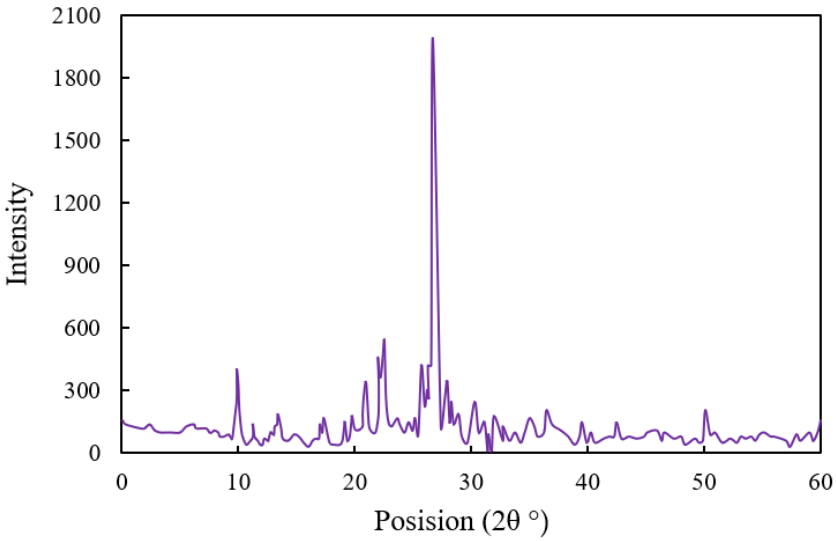

Figure 2. XRD patterns of natural zeolite (NZ).

Table 1. Chemical characteristics of the natural zeolite (NZ).

Constituent	Value %
SiO_2	70.46
Al_2O_3	13.74
Fe_2O_3	0.77
CaO	1.98
MgO	0.78
K_2O	2.82
SO_3	0.13
Na_2O	2.21

The natural zeolite (NZ) was initially crushed and then grinded to a size of less than 0.5 mm. To prepare the modified zeolite, 4 g of crude zeolite was mixed with 0.7289 g of hexadecyltrimethylammonium bromide, and stirred for 24 h at 21 °C. The modified zeolite was separated by centrifuging the solution at 100 rpm for 5 minutes. After 24 h, zeolite was filtered and washed with distilled water. The prepared mixture was dried in an oven for 24 h at 70 °C in the last step. The adsorbents were passed through a 0.5 mm sieve, and kept in a glass container for subsequent use in the adsorption tests. Figures 3 and 4 depict the surface morphology by SEM image and Energy Dispersive Atomic X-ray (EDAX) results of modified zeolite before cyanide adsorption.

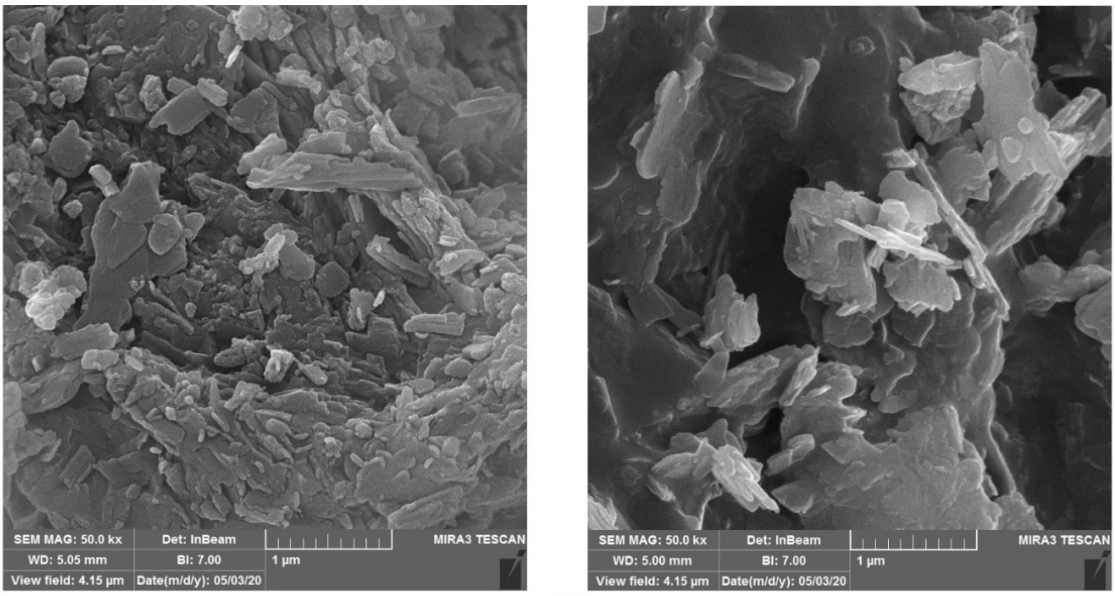

Figure 3. SEM images; A: Natural zeolite with a size ranging from 31 to 55 nm, B: Modified zeolite from 17 to 55 nm in diameter.

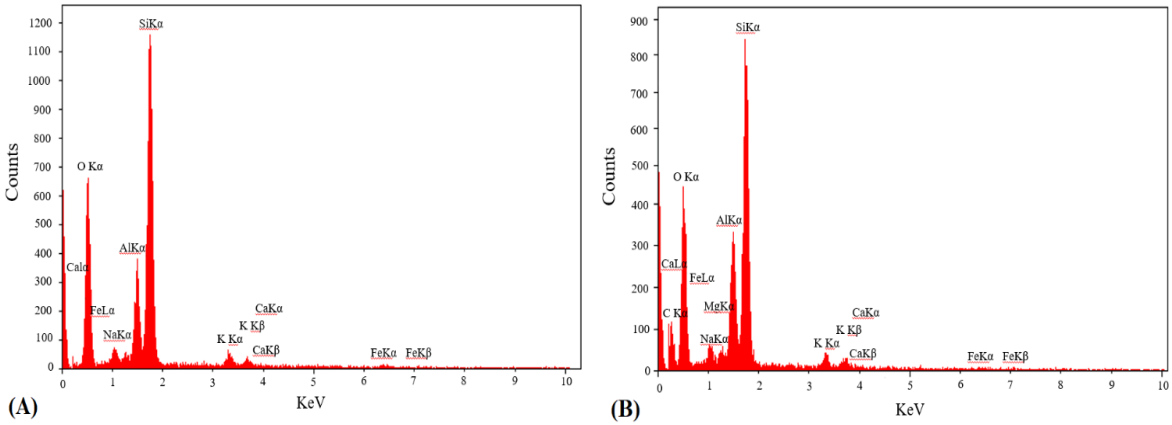

Figure 4. Energy dispersive X-ray analysis (EDAX) of zeolite; A: Before modifying, b: After modifying.

Figure 4 shows the surfactant adsorption on external surfaces of modified zeolite. The adsorbent particles were uniformly shaped of small particles (grey parts), ranging from 17 to 55 nm in diameter. After modifying zeolite with the surfactant contains carbon on its surface, which confirms the loading of HDTMA-Br carbon surfactants (see Figure 4). Figure 5 depicts data for the FT-IR spectrum of natural and modified zeolite. The spectrum detected at 400–4000 cm^{-1} shows the secondary building units of zeolitic structures such as double rings and pore opening [30]. The peaks that appeared at 1630–1640 and 3000–3700 cm^{-1} defined the existence of two bands. The first group corresponds to the bending vibration of H_2O molecules adsorbed on the natural and modified zeolite (1635 and 1635.74 cm^{-1}, respectively). For the second group, the bands at 3629.10 and 3446.27 cm^{-1} for natural zeolite and the broadband at 3629.86 and 3441.64 cm^{-1} for modified zeolite indicate the elongation vibration OH groups of the water molecules of the zeolite [31]. For the modified zeolite FT-IR, the two absorption bands at 2921.04 and 2852.12 cm^{-1} are attributed to asymmetric and symmetrical elongation vibrations of the methylene CH_2 group from the modified zeolite, which confirms the adsorption of the cationic surfactant on the zeolite surface [32].

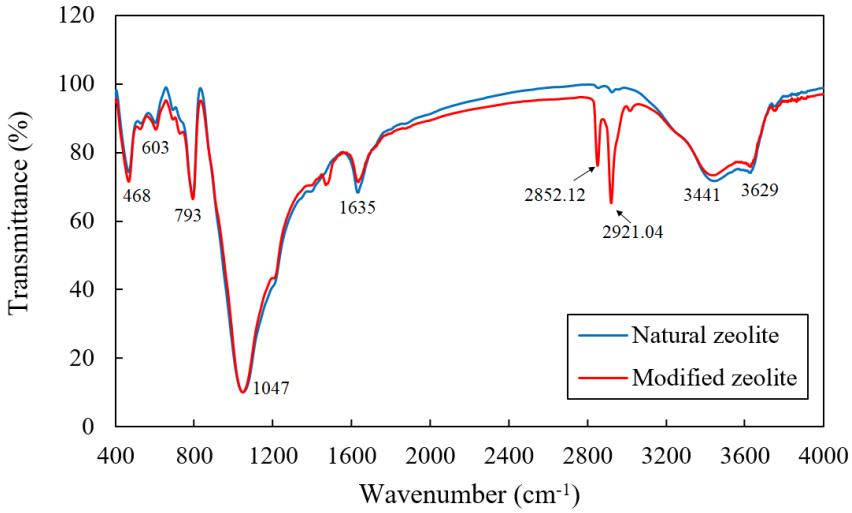

Figure 5. FT-IR spectra of natural and modified zeolite.

Table 2 presented the Brunauer–Emmet–Teller (BET) data of surface area analysis results for natural and modified zeolite. The BET plot analysis demonstrated that the modified adsorbent is a microporosity material with a surface area (3.41 m^2/g).

Table 2. BET data of natural and modified zeolite.

BET analyses	Natural zeolite	Modified zeolite
Pore size (nm)	31.89	30.51
Specific surface area (m^2/g)	7.68	3.41
Pore volume (cm^3/g)	0.061	0.026

2.3. Adsorption studies

The initial cyanide-containing solutions required for the experiment (1000 mg/L) were prepared by adding a certain amount of powdered sodium cyanide salt (NaCN) in deionized water and then diluted to the different practical concentrations (20–65 mg/L). Argentimetric titrations measured cyanide concentrations according to standard methods for examining water and wastewater (method 4500-CN-D [33]). For adsorption isotherm, 40 mL of solutions are diluted to the 20, 35, 45, and 65 mg/L concentrations by distilled water. The initial pH of cyanide solutions was 7 with ionic strength of 0.01 mol/L. The sodium chloride salt generated the ionic strength of the solution used. After providing the cyanide solution, 30 mg of natural and modified zeolite was added to 50 mL of these solutions. The samples were stirred for 24 hours at room temperature (21°C) at 100 rpm. After 5 minutes, the supernatant

was filtered through a filter paper (via 0.45 µm) and then centrifuged.

2.4. Experiments

All experiments were conducted at room temperature, except those meant for the effects of temperature study. Various experimental parameters such as pH (7, 8, 9 and 10), temperature (21, 30, 40 and 50 °C), initial cyanide concentration (10, 15, 20 and 35 mg/L), ionic strength (0.01, 0.05, 0.1 and 0.15 mol/L), and contact time (0–120 min) were investigated. In order to investigate the effect of the solution pH on the studied adsorbents, 40 mL of cyanide solution with a concentration of 20 mg/L was added to 4 flasks base solution with pHs of 7, 8, 9, and 10 and after adding of 0.6 g/L adsorbents of modified zeolite. Adjustment pH was performed using NaOH and HCl a normal. The test flasks were shaken at room temperature (21 °C) for 24 h. After 5 minutes, the supernatant was filtered through a filter paper (via 0.45 µm) and then centrifuged. To investigate the effect of ionic strength on cyanide adsorption, 40 mL of cyanide solution with a concentration of 20 mg/L was added to 4 flasks with a pH of 7 at 0.01, 0.05, 0.1, and 0.15 mol/L ion of the base solution created with sodium chloride was adding of 0.6 g/L adsorbents of modified zeolite. In order to investigate the effect of temperature and contact time on the studied adsorbents, in all experiments, the initial cyanide concentration, agitation time, and adsorbent of modified zeolite amount were in initial conditions, which had been determined with a concentration of 20 mg/L with a pH of 7 at 0.01 mol/L ion was adding of 0.6 g/L adsorbents of modified zeolite. The cyanide adsorbed in the solid phase was evaluated and calculated using the equation shown in Equation 1:

$$q_e = \frac{(C_o - C_e)V}{M} \quad (1)$$

where q_e (mg/g) is the equilibrium sodium cyanide (NaCN) concentration on adsorbent (mg/g), and C_e and C_o represent the equilibrium and initial concentrations of sodium cyanide (mg/L), respectively. M is the adsorbent weight (g) = 30g, and V is the solution volume (L) = 40 mL.

2.5. Adsorption in column analysis

Absorbent column experiments were performed in a glass cylinder with an inner diameter of 1.7 cm and a height of 50 cm, packed with sand as supporting layers at both ends was employed for the column experiments at room temperature (21 °C). 2 and 4 g of modified zeolite adsorbent was packed into the column to produce a 2 and 4 cm bed height (see Figure 6). Effects of process parameters like flow rates (0.25, 0.5, and 0.75 mL/min), bed depth (2 and 4 cm) with a constant concentration of 30 mg/L, and pH 8 were investigated. Samples were collected every half an hour from the bottom of the column, and were tested to know the lead concentration. The column performance was investigated by calculating the breakthrough time and uptake capacity. The column operation was halted when cyanide concentration in the effluent attained 100% of influent concentration.

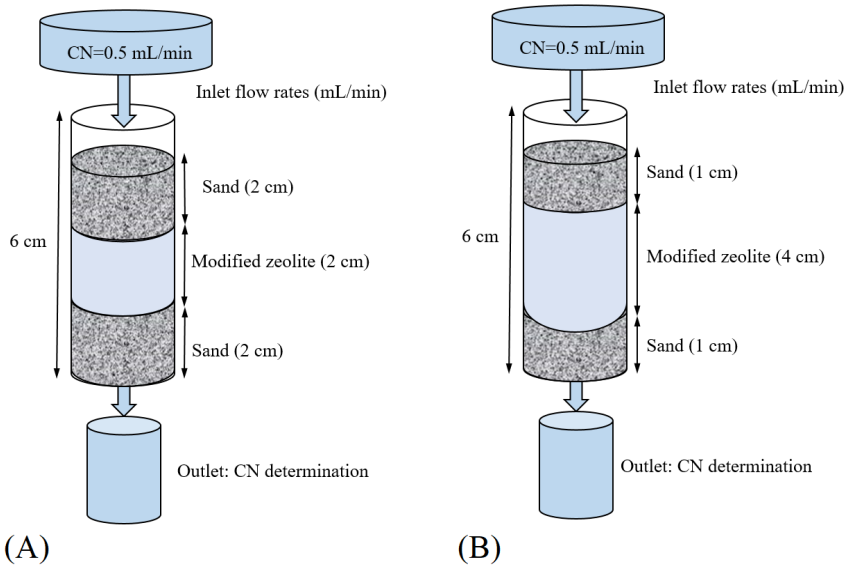

Figure 6. The schematic representation of the fixed-bed adsorption column for experimental study, A: Bed depth = 2 cm; B: Bed depth = 4 cm.

3. Results and Discussion

3.1. Effect of content time on adsorption

Results of cyanide uptake capacity of modified zeolite versus contact time in the cyanide solution are given in Figure 7. As displayed in this figure, in the first 60 min, the uptake of cyanide in the early adsorption stage was high and fast; after that, with the increase in the contact time, the uptake amount of the cyanide onto modified zeolite became almost stable for all the concentrations studied. Further contact time to over 60 min did not raise cyanide uptake, and the change in the removal rate remained poor. Adsorption of cyanide at the initial contact time is an interesting feature of the adsorbent for practical applications.

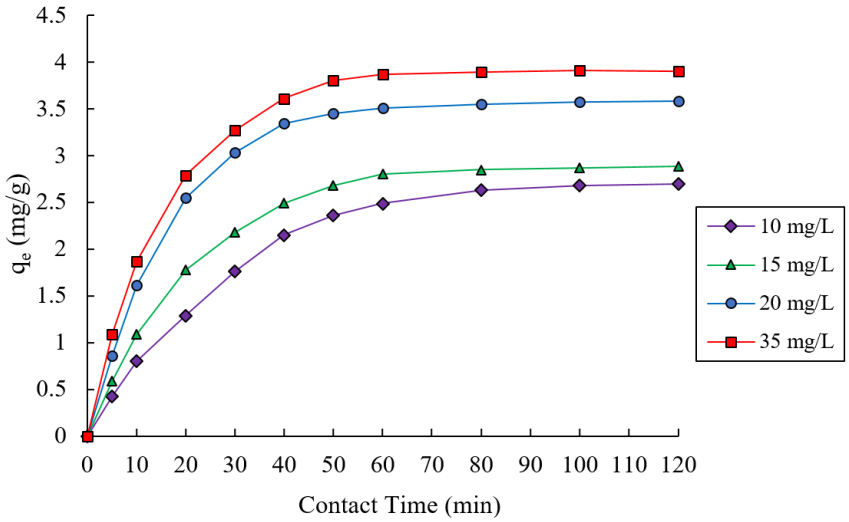

Figure 7. Effect of contact time on the cyanide adsorption (modified zeolite dosage: 30 g/40 mL; pH value: 7; temperature: 21°C).

3.2. Effect of pH on adsorption

The pH of the solution is one of the most important factors controlling the ion adsorption process on the adsorbent surface, which affects the properties of the contaminant, adsorption mechanism, and polarity of the adsorbent surface charge. At low pHs, cyanide ions are released as HCN gaseous [34], so the solution pH was implemented from pH 7–10 to investigate its effect on cyanide uptake (Figure 8). Results for modified types of zeolites showed that by increasing the pH value to 7 and 8, the cyanide adsorption increased and showed a maximum equilibrium uptake at pH = 8. Afterward, it was declined sharply with a further increase in pH and at pH equal to 10, with cyanide concentration 20 and 35 mg/L reaching its lowest amount 2.43 and 3.20 mg/g, respectively. The reason for the reduction in cyanide adsorption can be caused by the fact that at a higher pH (pH > 8), the attraction force between the cyanide molecules and zeolite's surface decreases, which cannot be removed by modified zeolite via ion exchange [25 and 35].

The results of this study did not confirm the previous findings [6]. They reported that the highest amount of cyanide uptake from solution by pistachio shell waste occurs in the pH range of 8-11.

3.3. Effects of temperature and initial cyanide concentration on adsorption

Temperature is an effective and important parameter in the cyanide removal process. Figure 9 represents the cyanide uptake capacity of modified zeolite as a function of initial cyanide concentration at different temperatures. It seems from the adsorption data that increases along with the increase in initial cyanide concentration in constant temperature. The increase in cyanide adsorption can be caused by a higher initial cyanide concentration supplied as a larger mass transfer driving force resulting from the concentration gradient [36]. Meanwhile, the cyanide uptake capacity onto modified zeolite increases as temperature increases. This result is because an endothermic process controls cyanide uptake from the modified zeolite. Therefore, with increasing temperature, the adsorption capacity of cyanide increased.

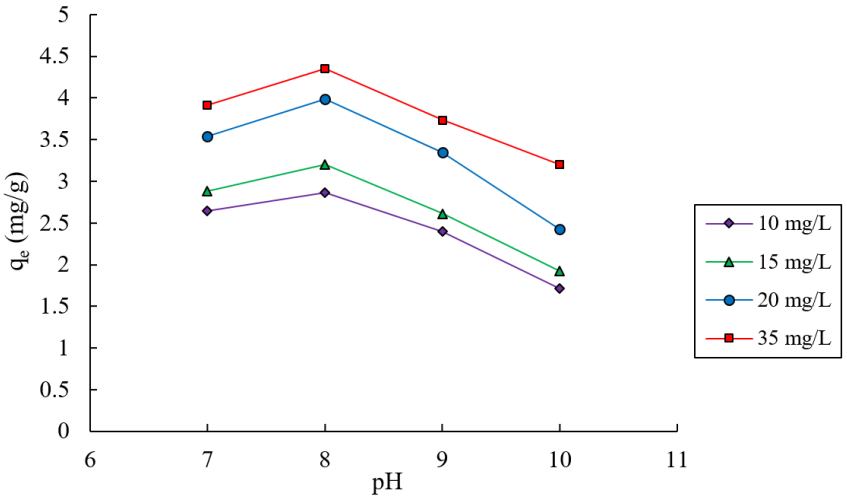

Figure 8. Influence of initial pH on the cyanide adsorption (modified zeolite dosage: 30 g/40 mL; initial cyanide concentration: 10 to 35 mg/L; temperature: 21°C).

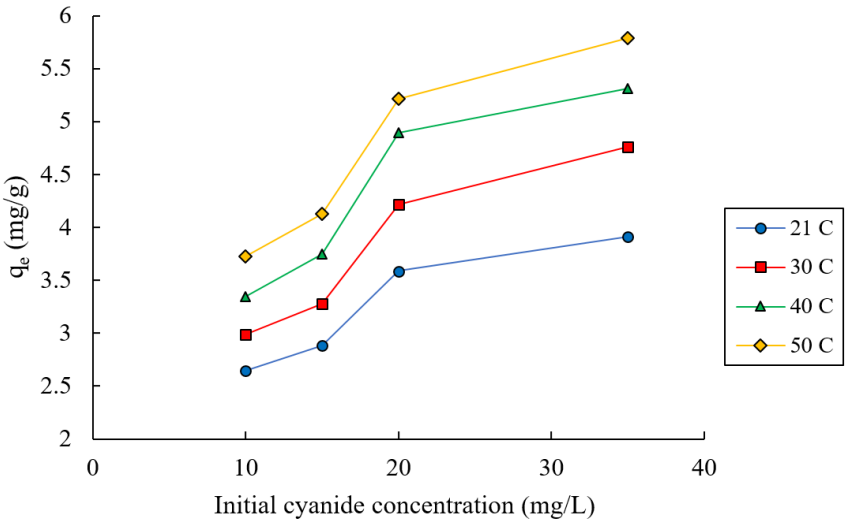

Figure 9, Influence of initial cyanide concentration on the cyanide adsorption in different temperatures (modified zeolite dosage: 30 g/40 mL; contact time: 120 min; pH value: 7.0).

3.4. Effect of ionic strength on cyanide adsorption

The ionic strength of the solution is one of the factors that affect the adsorption capacity. The effect of ionic strength on adsorption can be conveniently studied by adopting the inner/outer-sphere complexation model [37], synonymous with the electric double layer model [36]. The ionic strength of the solution at various cyanide concentrations is shown in Figure 10. For example, in constant concentrations, 20 mg/L, as the ionic strength was increased from 0.01 to 0.15 mol/L of sodium chloride, cyanide adsorption onto modified zeolite decreases from 3.57 to 1.7 mg/g. However, the cyanide uptake was increased when cyanide concentrations were increased from 10 to 35 mg/L. Increasing the ionic strength of the solution caused reduces the thickness of the electrical double layer and increases the concentration of anion in the sodium chloride; therefore, competition for adsorption on adsorption may have played a role in reducing cyanide adsorption.

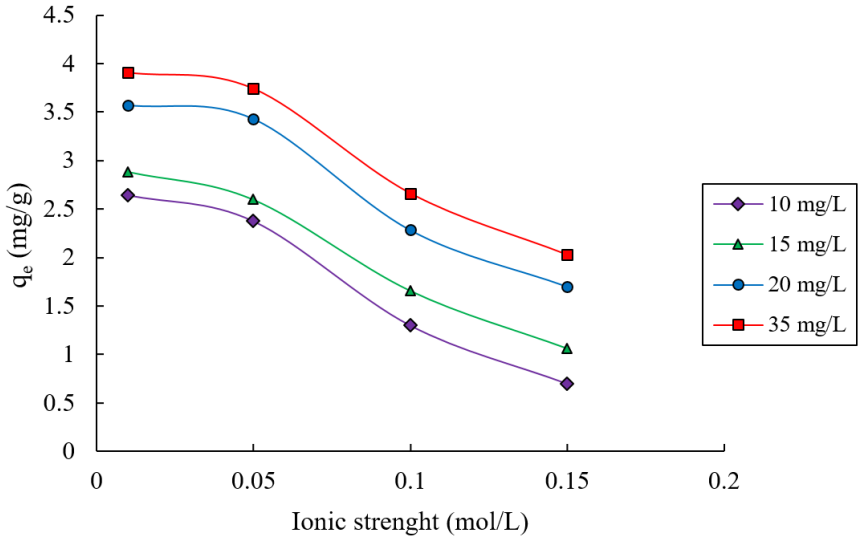

Figure 10. Influence of ionic strength on the cyanide adsorption (modified zeolite dosage: 30 g/40 mL; pH value: 7; temperature: 21°C).

3.5. Adsorption isotherm

The equilibrium adsorption isotherm is a helpful factor when it comes to the description of the mutually active behavior between solutes and adsorbents. It is also essential to lay the foundational ground for the design and operation process [38]. The batch procedure prepared adsorption isotherms for the cyanide containing natural and modified zeolite solutions. The isothermal tests were carried out in 40 mL of solutions with an initial cyanide concentration of 1 to 35 mg/L. The initial pH of 7 and ionic strength of 0.01 mol/L was added to 30 mg of naturally modified zeolite adsorbents in 50 mL test flasks. The adsorbent was shaken at 100 rpm at a specified temperature (21 °C) for all batch experiments. After shaking, the sample was filtered through a microporous membrane filter (0.45 µm). The solution was maintained at the desired pH by adding 0.01 mol/L of HCl or NaOH before commencing the adsorption experiment. The equilibrium data obtained was used to model the adsorption equilibrium by commonly used non-linear empirical models (Freundlich [39], Langmuir [40] and Tempkin [41]):

$$q_e = \frac{q_m K_L C_e}{1 + K_L C_e} \quad \text{Langmuir model} \quad (2)$$

$$q_e = K_F C_e^{1/n} \quad \text{Freundlich model} \quad (3)$$

$$q_e = B_T \ln K_T + B_T \ln C_e \quad \text{Tempkin model} \quad (4)$$

$$B_T = \frac{RT}{b_T} \quad (5)$$

where q_e (mg/g) and C_e (mg/L) are the equilibrium sodium cyanide concentrations in solid and liquid phases, respectively, q_m (mg/g) is the maximum adsorption capacity, R and T represent the gas constant (8.314 J/mol. °K) and absolute temperature (°K), and K_L, K_F, K_T, n, and b_T represents the equilibrium constants. As shown in Figure 11, natural and modified zeolite intensity of the absorption process decreased with increasing equilibrium cyanide concentration; this may be due to the reduction of adsorption sites for cyanide on the adsorbent surface. The intensity of the cyanide adsorption process on modified zeolite is higher than natural zeolite. Natural zeolite and modified zeolite's maximum adsorption cyanide capacity were 0.54 and 3.97 mg/g, respectively. The results calculated for each model and the corresponding parameters are listed in Table 3. The validation of adsorption isotherm models was measured by determining the two mathematical parameters: the regression coefficient (R^2) and the variance deviation between experimental values of q_e and models' prediction of q_e.

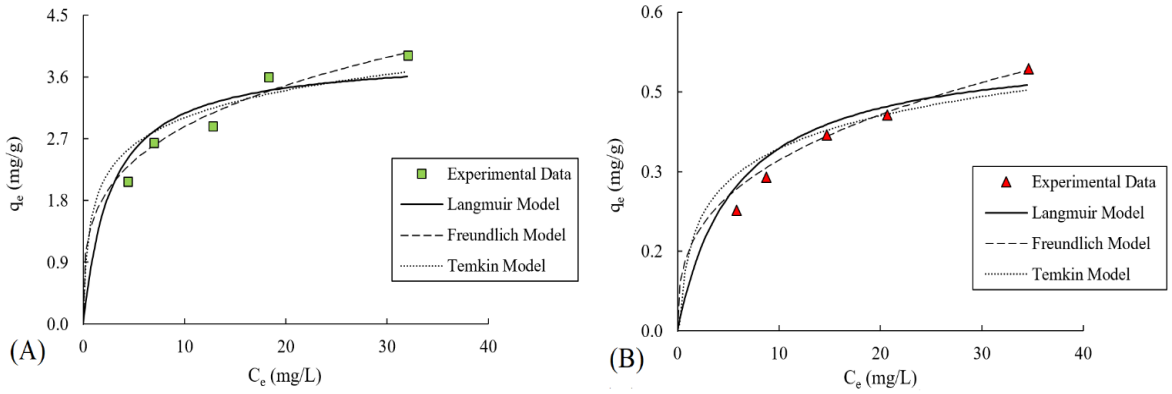

Figure 11. Adsorption isotherm plots for cyanide uptake on the A: modified zeolite and B: natural zeolite.

Table 3. Isotherm constants and regression data of adsorption isotherms of cyanide on the natural and modified zeolite.

Adsorbent	Models	Parameters			
		K_L	q_m	R^2	Variance
Natural zeolite	Langmuir	0.18	0.54	0.92	0.054
Modified zeolite		0.37	3.97	0.93	0.418
Adsorbent	**Models**	**K_F**	**1/n**	**R^2**	**Variance**
Natural zeolite	Freundlich	0.15	0.34	0.97	0.03
Modified zeolite		1.53	0.27	0.98	0.15
Adsorbent	**Models**	**K_T**	**A**	**R^2**	**Variance**
Natural zeolite	Tempkin	27216	4.68	0.93	0.04
Modified zeolite		4234	18.88	0.95	0.28

From this Table, it seems that the cyanide adsorption by natural and modified zeolite follows the Langmuir, Freundlich, and Tamkin adsorption models. The separation factor (R_L) was estimated from the following equation [42]:

$$R_L = \frac{1}{(1 + K_L C_i)} \quad (6)$$

Here, K_L (L/mg) refers to the Langmuir constant, and C_i is denoted to the adsorbate initial concentration (mg/L). When the R_L value is less than unity, the adsorption is considered favorable, and when greater than unity is considered unfavorable. Also when R_L is equal to 0, the adsorption is irreversible, and the unity value represents the adsorption's linearity. The values of R_L in the present investigation have been found in the range 0.07~0.31, depicting that cyanide adsorption is favorable.

3.6. Adsorption kinetics

For adsorption, kinetics tests were carried out in 40 mL of solutions with an initial cyanide concentration of 20 mg/L sodium chloride base solution, and pH 7 to 0.03 g of modified zeolite was added to 50 mL test flasks. The test flasks were quenched at 5, 15, 30, 60, 120, 180, 240, 480, and 960 minutes at room temperature (21 °C). Then the clear supernatant was transferred to filter papers and centrifuged for 5 min. The adsorption systems' kinetic was studied using the pseudo-first-order and pseudo-second-order models. The pseudo-first and second-order kinetic model of Lagergren [43] and Ho and McKay [44] are presented in Equations 7 and 8:

$$\ln(q_e - q_t) = \ln q_e - K_1 t \quad (7)$$

$$t / q_t' = 1 / K_2 q_e'^2 + 1(t) / q_e' \quad (8)$$

q_e is the quantity adsorbed at equilibrium (mg/g), and q_t is the quantity absorbed at time t (mg/g). K_1 is the rate constant for the pseudo-first-order sorption (min^{-1}). K_2 is the rate constant of the pseudo-second-order kinetic equation in g/mg min^{-1}, q'_e is the maximum sorption capacity in mg/g, and q'_t (mg/g) is the amount of sorption at time t. Figure 12 shows the plotted models including the pseudo-first and second-order kinetic models with experimental data from the present study. The extracted kinetic information is consolidated in Table 4.

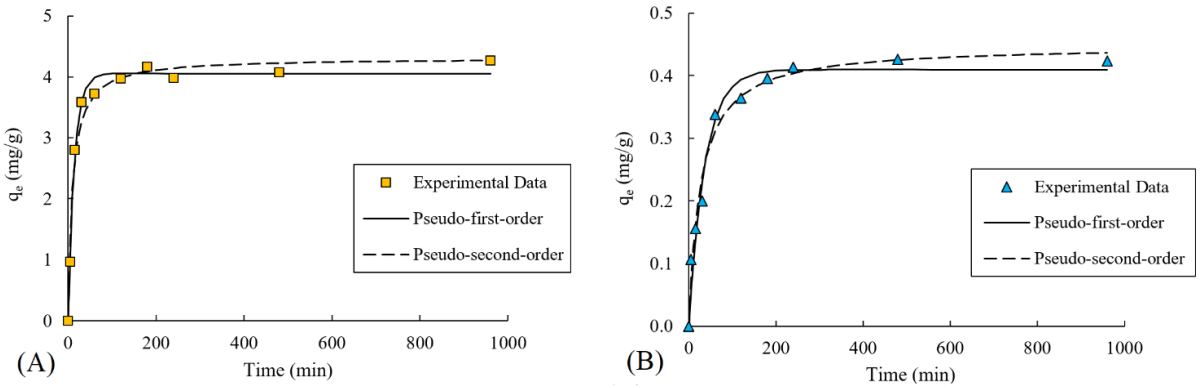

Figure 12. Kinetic isotherm plots for cyanide uptake on the A: modified zeolite, B: natural zeolite.

The cyanide adsorption kinetics on natural and modified zeolites did not differ much between the pseudo-first and second-order models. The values q_e obtained from the experimental and calculated data were slightly different. Modified zeolite had a higher adsorption capacity and reaction rate than natural zeolite. In this regard, it can be said that in natural zeolite, perhaps only the outer surface of the adsorbent is used as adsorption sites. However, about the modified zeolite and the outer surface, the internal parts of the adsorbent also participated in the adsorption. Hence, the adsorption capacity of cyanide increased with the modified zeolite. On the other hand, the absorption rate also increases due to the physical nature of absorption.

Table 4. Kinetic details of cyanide adsorption onto the natural and modified zeolite.

Adsorbent	Models	Parameters			
		K_1	q_e	R^2	Variance
Natural zeolite	Pseudo-first	0.03	0.41	0.97	0.03
Modified zeolite	order	0.07	3.65	0.98	0.16
Adsorbent	**Models**	**K_2**	**q_e**	**R^2**	**Variance**
Natural zeolite	Pseudo-second	0.08	0.45	0.98	0.02
Modified zeolite	order	0.03	3.88	0.97	0.23

According to Figure 12 and Table 4, the pseudo-first-order and the pseudo-second-order model showed a good ability to simulate and describe the kinetics of cyanide adsorption by surfactant-modified zeolite. This means that tiny pores or active sites above the adsorbent surface are responsible for the adsorption phenomenon. On the other hand, the pseudo-second-order model indicated that the kinetics of cyanide adsorption is controlled by chemical adsorption [45]. In general, according to the results of this study, the combination of chemical and electrostatic adsorption is involved in the adsorption of cyanide by natural and modified zeolite.

3.7. Column study

The breakthrough curves of the column adsorption process at different flow rates and bed heights were investigated. Yoon and Nelson's model [46], which developed a relatively simple theoretical model, is also applied to check the experimental data. The theory of this model is: the reduction rate in the adsorption of each adsorbate molecule is proportional to the breakthrough curves, and the adsorption on the adsorbent is considered. Yoon and Nelson [46] model is expressed as:

$$\ln\left(\frac{C_t}{C_0 - C_t}\right) = k_{YN}t - \tau k_{YN} \quad (9)$$

where τ is the breakthrough time required for 50% adsorbate breakthrough (min), t is the sampling time (min), and k_{YN} is the rate constant (min^{-1}). The constant values of k_{YN} and τ can be calculated by the linear plot of ln ($C_t/(C_0 - C_t)$) against time. Figure 13 shows a typical S-shape graph, known as a breakthrough curve, obtained for cyanide adsorption on modified zeolite for different flow rates of 0.25, 0.5, and 0.75 mL/min, at bed height of 4 cm and pH of 8. The breakthrough time for cyanide adsorption onto modified zeolite increases with the decreasing flow rate from 0.75 to 0.25 mL/min. In other words, the breakthrough time is prolonged with the decreased

flow rate, indicating a longer column life with a longer contact time. The modified zeolite column quickly reaches its maximum capacity at a higher flow rate. The effect of bed heights of 2 and 4 cm (corresponding to 2 and 4 g of adsorbent) on the cyanide adsorption in the column was investigated at a constant flow rate of 0.5 mL/min. The adsorption breakthrough curves obtained at different bed heights are shown in Figure 14. As expected in the conditions used, the breakthrough time is improved by the 2 cm bed in favor of cyanide removal with modified zeolite.

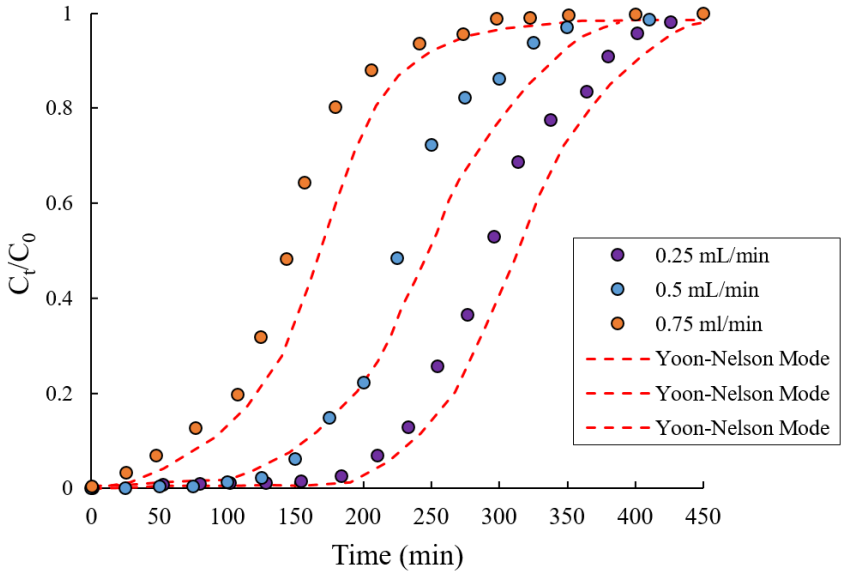

Figure 13. Effect of flow rate on the breakthrough curve of cyanide adsorption in the column (Bed height: 4 cm; pH value: 8; temperature: 21˚C).

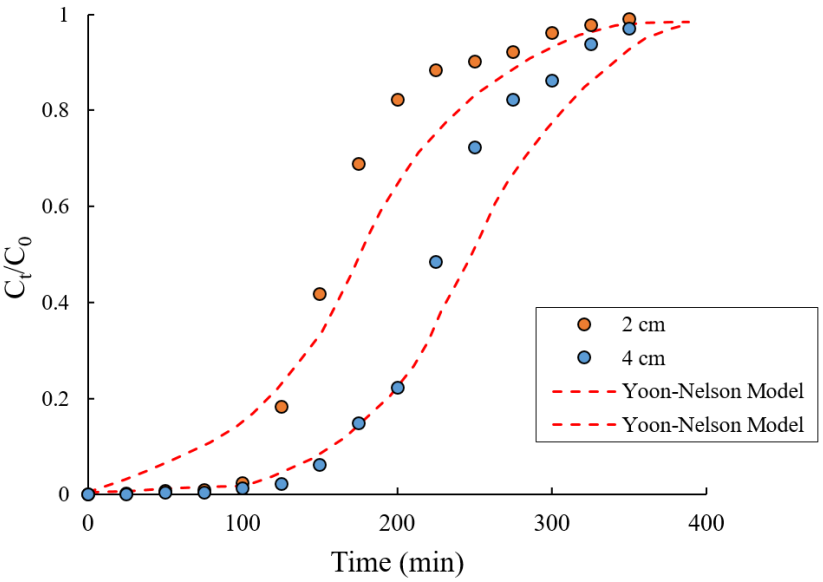

Figure 14. Effect of bed height on the breakthrough curve of cyanide adsorption in the column. (Flow rate: 0.5 mL/min; pH value: 8; temperature: 21˚C).

The results for Yoon-Nelson parameters and related coefficients of correlation and R^2 values are shown in Table 5. Comparisons of the predicted model's curve and the experimental curve in these figures show that predicted Yoon-Nelson curves are closer to experimental curves. Also high R^2 values show a good model fitting to the experimental data.

Table 5. Parameters of Yoon-Nelson model under column adsorption process.

C_0 (mg/L)	Q (mL/min)	Z (cm)	pH	Yoon-Nelson model		
				k_{YN} (min^{-1})*10^{-2}	τ (min)	R^2
5	0.25	4	8	1.26	321.15	0.963
5	0.5	4	8	1.14	252.79	0.961
5	0.75	4	8	1.04	174.53	0.958
5	0.5	2	8	1.09	176.85	0.965

4. Conclusions

The study concludes that surfactant-modified zeolite is an effective and feasible method as an adsorbent to adsorb cyanide. The performance for cyanide uptake of modified zeolite depends on the contact time, initial cyanide concentration, temperature, and pH value. Cyanide removal decreased with increasing pH and ionic strength due to the negative charge of the modified zeolite surface. It increased with an increase in initial cyanide concentration and solution temperature.

The Langmuir, Freundlich, and Tamkin adsorption models showed an acceptable ability to characterize the cyanide adsorption isotherm using raw and surfactant-modified zeolite (Freundlich model was most consistent with the experimental data).

The adsorption capacity of cyanide by modified zeolite was 3.97 mg/g, significantly increased compared to the maximum adsorption capacity of natural zeolite cyanide (0.54 mg/g). The adsorption kinetics results showed that the pseudo-first-order and pseudo-second-order models have an excellent ability to describe the adsorption kinetics of cyanide contaminants using natural and modified zeolites.

Cyanide uptake through a fixed-bed column depended on the bed depth and flow rate. Breakthrough time increases with a higher bed depth and a lower flow rate. The maximum adsorption capacity was at a lower flow rate due to high contact time and higher bed depth. Yoon-Nelson model was successfully used to predict the breakthrough curves, indicating that it was very suitable for surfactant-modified zeolite column design.

In general, the results showed that surfactant-modified zeolite could be used as a non-toxic and effective adsorbent on a laboratory scale and in the bed of Zareshoran gold mine tailings dams due to economic and environmental considerations in removing cyanide from aqueous media.

References

[1]. Ghasemi, N. and Rohani, S., 2019. Optimization of cyanide removal from wastewaters using a new nano-adsorbent containing ZnO nanoparticles and MOF/Cu and evaluating its efficacy and prediction of experimental results with artificial neural networks. *Journal of Molecular Liquids, 285*, 252-269.

[2]. Han, B., Shen, Z., Wickramasinghe, S.R. 2005. Cyanide removal from industrial wastewaters using gas membranes. *Journal of membrane science, 257*(1), 171-181.

[3]. Logsdon, M.J., Hagelstein, K., Mudder, T. 1999. The management of cyanide in gold extraction: International Council on Metals and the Environment, *Ottawa*.

[4]. Lee, T. Y., Kwon, Y. S., and Kim, D. S. (2004). Oxidative treatment of cyanide in wastewater using hydrogen peroxide and homogeneous catalyst. *Journal of Environmental Science and Health, Part A*, *39*(3), 787-801.

[5]. Amaouche, H., Chergui, S., Halet, F., Yeddou, A. R., Chergui, A., Nadjemi, B., and Ould-Dris, A. (2019). Removal of cyanide in aqueous solution by oxidation with hydrogen peroxide catalyzed by copper oxide. *Water Science and Technology*, *80*(1), 126-133.

[6]. Moussavi, G. and Khosravi, R., 2010. Removal of cyanide from wastewater by adsorption onto pistachio hull wastes: Parametric experiments, kinetics and equilibrium analysis. *Journal of Hazardous Materials, 183*(1-3), 724-730. https://doi.org/10.1016/j.jhazmat.2010.07.086.

[7]. Gebresemati, M., Gabbiye, N., and Sahu, O. 2017. Sorption of cyanide from aqueous medium by coffee husk: Response surface methodology. *Journal of applied research and Technology*, *15*(1), 27-35.

[8]. Osathaphan, K., Boonpitak, T., Laopirojana, T., and Sharma, V. K. 2008. Removal of cyanide and zinc–cyanide complex by an ion-exchange process. *Water, air, and soil pollution*, *194*(1), 179-183.

[9]. Simsek, H., Kobya, M., Khan, E., and Bezbaruah, A. N. 2015. Removal of aqueous cyanide with strongly basic ion-exchange resin. *Environmental technology*, *36*(13), 1612-1622.

[10]. Zhang, J., Liu, L., Liang, Y., Zhou, J., Xu, Y., Ruan, X., Lu, Y., Xu, Z., Qian, G. 2015. Enhanced precipitation of cyanide from electroplating wastewater via self-assembly of bimetal cyanide complex. *Separation and Purification Technology*, *150*, 179-185.

[11]. Bodalo-Santoyo, A., Gómez-Carrasco, J. L., Gomez-Gomez, E., Maximo-Martin, F., and Hidalgo-Montesinos, A. M. 2003. Application of reverse osmosis to reduce pollutants present in industrial wastewater. *Desalination*, *155*(2), 101-108.

[12]. Vasquez Salazar, E. E. and Hurtado Bolanos, F. P. 2021. Cyanide compounds removal efficiency in a reverse osmosis system using a water supply from a co-precipitation chemical process. *Desalination and Water Treatment*, *229*, 235-242.

[13]. Jaszczak, E., Polkowska, Z., Narkowicz, S., Namieśnik, J., 2017. Cyanides in the environment analysis problems and challenges. *Environmental Science and Polluion Research, 24*, 15929–15948.

[14]. Naeem, S., Zafar, U. 2009. Adsorption studies of cyanide (CN)- on alumina, *PAKISTAN JOURNAL OF ANALYTICAL & ENVIRONMENTAL CHEMISTRY,10*, 83–87.

[15]. Adhoum, N. and Monser, L. 2002. Removal of cyanide from aqueous solution using impregnated activated carbon. *Chemical Engineering and Processing: Process Intensification*, *41*(1), 17-21.

[16]. Halet, F., Yeddou, A. R., Chergui, A., Chergui, S., Nadjemi, B., and Ould-Dris, A. 2015. Removal of cyanide from aqueous solutions by adsorption on activated carbon prepared from lignocellulosic by-products. *Journal of Dispersion Science and Technology*, *36*(12), 1736-1741.

[17]. Wang, X., Wang, X., Tan, H., Hu, Z., Deng, S., and Li, Y. 2015. Removal of hydrogen cyanide by using activated carbon: the effect of adsorption condition and chemical modification. *Journal of Biobased Materials and Bioenergy*, *9*(6), 545-552.

[18]. Depci, T. 2012. Comparison of activated carbon and iron impregnated activated carbon derived from Gölbaşı lignite to remove cyanide from water. *Chemical Engineering Journal*, *181*, 467-478.

[19]. Alonso-González, O., Nava-Alonso, F., and Uribe-Salas, A. 2009. Copper removal from cyanide solutions by acidification. *Minerals Engineering*, *22*(4), 324-329.

[20]. Bae, M., Lee, H., Kim, S., and Yoo, K. 2019. Destruction of cyanide and removal of copper from waste printed circuit boards leach solution using electro-generated hypochlorite followed by magnetite adsorption. *Metals*, *9*(9), 963.

[21]. Tyagi, M., Rana, A., Kumari, S., and Jagadevan, S. 2018. Adsorptive removal of cyanide from coke oven wastewater onto zero-valent iron: Optimization through response surface methodology, isotherm and kinetic studies. *Journal of Cleaner Production*, *178*, 398-407.

[22]. Coronel, S., Endara, D., Lozada, A. B., Manangón-Perugachi, L. E., and de la Torre, E. 2021. Photocatalytic Study of Cyanide Oxidation Using Titanium Dioxide (TiO2)-Activated Carbon Composites in a Continuous Flow Photo-Reactor. *Catalysts*, *11*(8), 924.

[23]. Samarghandi, M. R., Al-Musawi, T. J., Mohseni-Bandpi, A., and Zarrabi, M. 2015. Adsorption of cephalexin from aqueous solution using natural zeolite and zeolite coated with manganese oxide nanoparticles. *Journal of molecular liquids*, *211*, 431-441.

[24]. Mohseni-Bandpi, A., Al-Musawi, T. J., Ghahramani, E., Zarrabi, M., Mohebi, S., and Vahed, S. A. 2016. Improvement of zeolite adsorption capacity for cephalexin by coating with magnetic Fe_3O_4 nanoparticles. *Journal of Molecular Liquids*, *218*, 615-624.

[25]. Noroozi, R., Al-Musawi, T. J., Kazemian, H., Kalhori, E. M., and Zarrabi, M. 2018. Removal of cyanide using surface-modified Linde Type-A zeolite nanoparticles as an efficient and eco-friendly material. *Journal of Water Process Engineering*, *21*, 44-51.

[26]. Torabian, A., Kazemian, H., Seifi, L., Bidhendi, G.N., Azimi, A.A., Ghadiri, S.K., 2010. Removal of petroleum aromatic hydrocarbons by surfactant-modified natural zeolite: the effect of surfactant. *Clean Soil, Air, Water, 38*(1), 77-83. https://doi.org/10.1002/clen.200900157.

[27]. Ashrafizadeh, S.N., Khorasani, Z., Gorjiara, M., 2008. Ammonia removal from aqueous solutions by Iranian natural zeolite. *Separation Science and Technology, 43*(4), 960-978. https://doi.org/10.1080/01496390701870614

[28]. Manyuchi, M. M., Sukdeo, N., and Stinner, W. 2022. Potential to remove heavy metals and cyanide from gold mining wastewater using biochar. *Physics and Chemistry of the Earth, Parts A/B/C*, *126*, 103110.

[29]. Zhou, S., Li, W., Liu, W., and Zhai, J. 2023. Removal of metal ions from cyanide gold extraction wastewater by alkaline ion-exchange fibers. *Hydrometallurgy*, *215*, 105992. https://doi.org/10.1016/j.hydromet.2022.105992.

[30]. Bukhari, S. S., Behin, J., Kazemian, H., and Rohani, S. 2015. Synthesis of zeolite NA-A using single mode microwave irradiation at atmospheric pressure: The effect of microwave power. *The Canadian Journal of Chemical Engineering*, *93*(6), 1081-1090.

[31]. Larsen OFA and Woutersen S. 2004. Vibrational relaxation of the H2O bending mode in liquid water. *J Chem Phys*. *121*, 12143–12145.

[32]. Taffarel, S. R. and Rubio, J. 2010. Adsorption of sodium dodecyl benzene sulfonate from aqueous solution using a modified natural zeolite with CTAB. *Minerals Engineering*, *23*(10), 771-779.

[33]. Apha, A. 2005. Wpcf. Standard methods for the examination of water and wastewater. *20th Ed.,Washington, DC*.

[34]. Eletta, O.A.A., Ajayi, O.A., Ogunleye, O.O., and Akpan, I.C., 2016. Adsorption of cyanide from aqueous solution using calcinated eggshells: Equilibrium and optimization studies. *Journal of Environmental Chemical Engineering*, *4*(1), 1367-1375.

[35]. Deveci, H. A. C. I., Yazıcı, E. Y., Alp, I., and Uslu, T. U. N. C. A. Y. 2006. Removal of cyanide from aqueous solutions by plain and metal-impregnated granular activated carbons. *International Journal of mineral processing*, *79*(3), 198-208.

[36]. Stavropoulos, G.G., Skodras, G.S., and Papadimitriou, K.G., 2015. Effect of solution chemistry on cyanide adsorption in activated carbon. *Applied thermal engineering, 74*,. 182-185. https://doi.org/10.1016/j.applthermaleng.2013.09.060.

[37]. Liu, G. J., Zhang, X. R., McWilliams, L., Talley, J. W., and Neal, C. R. 2008. Influence of ionic strength, electrolyte type, and NOM on As (V) adsorption onto TiO2. *Journal of Environmental Science and Health Part A*, *43*(4), 430-436.

[38]. Li, C., Yu, Y., Zhang, Q., Zhong, H., and Wang, S. 2020. Removal of Ammonium from Aqueous Solutions using Zeolite Synthesized from Electrolytic Manganese Residue. *International Journal of Chemical Engineering*, *2020*.

[39]. Freundlich, H. M. F. 1906. Over the adsorption in solution. *J. Phys. chem*, *57*(385471), 1100-1107.

[40]. Langmuir, I. 1916. The constitution and fundamental properties of solids and liquids. Part I. Solids. *Journal of the American chemical society*, *38*(11), 2221-2295.

[41]. Tempkin, M. I. and Pyzhev, V. J. A. P. C. 1940. Kinetics of ammonia synthesis on promoted iron catalyst. *Acta Physicochimica URSS*, *12*(1), 327.

[42]. Weber, T. W. and Chakravorti, R. K. 1974. Pore and solid diffusion model for fixed bed adsorbents. *AIChE Journal, 20*, 228.

[43]. Lagergren, S. K. 1898. About the theory of so-called adsorption of soluble substances. *Sven. Vetenskapsakad. Handingarl*, *24*, 1-39.

[44]. Ho, Y. S. and McKay, G. 1999. Pseudo-second order model for sorption processes. *Process biochemistry*, *34*(5), 451-465.

[45]. Kumar, P.S. and Kirthika, K. 2009. Equilibrium and kinetic study of adsorption of nickel from aqueous solution onto bael tree leaf powder. *Journal of Engineering Science and Technology, 4*(4), 351-363.

[46]. Yoon, Y. H. and Nelson, J. H. 1984. Application of gas adsorp-tion kinetics I. A theoretical model for respirator cartridge servicelife. *American Industrial Hygiene Association Journal, 45*(8), 509–516.

حذف سیانید از دوغاب باطله کارخانه فرآوری طلا توسط زئولیت اصلاح شده با سورفکتانت

مهدی سلیمانی قره گل[۱]، کاظم بدو[۱]، بهزاد نعمتی اخگر[۲*]

۱- گروه مهندسی عمران، دانشکده فنی و مهندسی، دانشگاه ارومیه، ارومیه، ایران

۲- گروه مهندسی معدن، دانشکده فنی و مهندسی، دانشگاه ارومیه، ارومیه، ایران

ارسال ۲۰۲۳/۰۶/۰۳، پذیرش ۲۰۲۳/۱۱/۰۱

* نویسنده مسئول مکاتبات: b.n.akhgar@urmia.ac.ir

چکیده:

این مقاله به موضوع بررسی حذف سیانید از محلول‌های آبی با استفاده از زئولیت فعال شده توسط هگزا دسیل تری متیل آمونیوم برماید می‌پردازد. پس از تعیین ویژگی‌های جاذب تهیه شده توسط روشهای XRD، SEM، FTIR و BET، تاثیر متغیرهایی مانند غلظت ابتدایی سیانید، pH، زمان تماس، دما و قدرت یونی سیانید با انجام آزمایش‌های ناپیوسته و تاثیر ضخامت بستر و نرخ جریان بر روی میزان جذب سیانید به روش ستونی مورد سنجش قرار گرفت. آزمایش XRD نشان داد که زئولیت اولیه مورد استفاده حاوی کانی کلینوپتیلولایت است و پوشش سطحی زئولیت اولیه توسط سورفکتانت به روش SEM مورد شناسایی قرار گرفت. نتایج FT-IR جذب سورفکتانت کاتیونی بر روی سطح اصلاح شده زئولیت را تایید می‌کند. مدل‌های جذب لانگمیور، فرندلیچ و تمکین قابلیت قابل توجهی در توصیف ایزوترم جذب سیانید با استفاده از جاذب مورد مطالعه از خود نشان داده‌اند. ظرفیت جذبی سیانید توسط زئولیت اصلاح شده ۳/۹۷ mg/g بود که بصورت چشمگیری نسبت به ظرفیت جذب حداکثری سیانید توسط زئولیت اولیه (۰/۵۴ mg/g) افزایش یافته است. سینتیک جذب این آلاینده‌های سیانیدی توسط زئولیت اولیه و اصلاح شده بخوبی با استفاده از مدل شبه درجه دو قابل توصیف می‌باشد. حداکثر جذب سیانید در pH برابر هشت بدست آمد. حذف سیانید با افزایش pH و قدرت یونی محلول اصلی کاهش و با بیشتر شدن دما افزایش یافت. نتایج مطالعات ستونی افزایش ظرفیت جذب با افزایش ضخامت بستر و کاهش ظرفیت جذب در اثر افزایش نرخ جریان را مورد تایید قرار داد. منحنی یون-نلسون با مقدار R^2 بالایی به منحنی های آزمایشی نزدیک هستند.

کلمات کلیدی: سیانید، سورفکتانت، ایزوترم جذب، سینتیک، سد باطله طلا.